

The Inelastic Mean Free Paths of Electrons in Semiconducting III-V Compounds*

C. M. Kwei and L. W. Chen

Department of Electronics Engineering, National Chiao Tung University, Hsinchu, Taiwan 300, Republic of China.

The inelastic mean free path of electrons in solids is an important parameter in surface studies using AES and XPS. In this paper we present theoretical calculations of this parameter for the semiconducting III-V compounds GaAs, GaSb, GaP, InSb and InAs. These calculations are based on a model dielectric function for the response of the valence band and the local-plasma-approximation for the response of inner shells. In the former case, the Kramers-Kronig relation and the partial sum rule for valence electrons are applied. In the latter case, the electron density distribution obtained from the Hartree-Slater model is utilized. Results are compared to other calculations using the Penn's model and the model of Ashley *et al.* for GaAs. Since no data on experimental electron attenuation lengths in the important semiconducting III-V compounds are available, it is suggested that direct calculations of the present type are useful in applications.

INTRODUCTION

The electron inelastic mean free path is an important parameter in surface studies using Auger electron spectroscopy (AES) and x-ray photoelectron spectroscopy (XPS). Although experimental^{1,2} and theoretical³⁻⁵ data regarding this parameter over a fairly wide range of electron energies in various media are available in the literature, very little work has been done with respect to such data in the important media of semiconducting III-V compounds. Part of the reason from the theoretical point of view is the difficulty involved in treating the large number of inner shells.

A few theoretical models are available for the calculations of electron inelastic mean free paths in many elements and compounds. Among these, the works of Tung *et al.*⁶ and Penn⁷ are often cited. Both of these works have utilized the electron-gas model to describe the response of all electrons in the materials. Although the electron-gas model is a good approximation for the so-called free-electron-like materials having a simple energy loss spectrum with a single, dominant plasmon peak, the model is not good for those materials which have more complex energy loss spectra such as semiconducting III-V compounds.⁴ In order to obtain more accurate estimates about the inelastic mean free paths, one needs to make use of experimental optical data which contain the actual response information of valence electrons. The contribution to the inelastic mean free path from core electrons is less important than that of valence electrons. A simple treatment which takes into consideration the electron density distribution of individual inner shells and satisfies the basic sum rule is quite enough.

In this paper we have calculated the inelastic mean free paths of electrons in the III-V compounds for electron energies less than 10 keV. Our approach invol-

ved the use of appropriate models to describe the inelastic interactions of energetic electrons with the valence band and with the inner shells of III-V compounds. In the case of the valence band, we have employed a model dielectric function based on the Drude-type expression but generalized to make it compatible with the response function for the III-V compounds. Parameters in the model dielectric function were determined by a fit of the theoretical imaginary part of this function to the available experimental data in the optical limit. The calculated energy loss function was subsequently checked with the corresponding experimental results. For inner shells, we have applied the local-plasma-approximation⁸ and the Hartree-Slater electron density distribution⁹ for the calculation of differential and total ionization cross-sections. The validity of the local-plasma-approximation to the tightly bound inner shells has been verified in several other applications.¹⁰⁻¹²

VALENCE BAND

The contribution of the valence band to the inverse mean free path of electrons is given by¹³

$$\mu_v(E) = \frac{1}{\pi E} \int_0^E d\omega \int_{k_-}^{k_+} \frac{dk}{k} \text{Im} \left[-\frac{1}{\varepsilon(k, \omega)} \right], \quad (1)$$

where $\text{Im}[-1/\varepsilon(k, \omega)]$ is the energy loss function of the medium, $\varepsilon(k, \omega)$ is the complex dielectric function of the medium as a function of momentum transfer k and energy transfer ω , $k_{\pm} = \sqrt{2E} \pm \sqrt{2E - 2\omega}$ are obtained from the energy-momentum conservation relations, and E is the energy of incident electrons. Note that all quantities and equations are expressed in atomic units in this paper.

The model dielectric function used in this paper is identical to that used previously.¹² It will be restated briefly here for the convenience of the users. The imaginary part of the dielectric function in the limit of zero momentum transfer is assumed to be a sum of

* Research sponsored by the National Science Council of the Republic of China.

Paper presented at the Quantitative Surface Analysis (QSA-4) Conference, Teddington UK, November 1986.

Drude type terms:¹⁴

$$\epsilon_2(0, \omega) = \sum_i \frac{A_i \gamma_i \omega}{(\omega^2 - \omega_i^2)^2 + \omega^2 \gamma_i^2}, \quad (2)$$

where A_i , γ_i , and ω_i are, respectively, the oscillator strength, damping constant, and eigenenergy associated with the i th group of electrons in the valence band of III-V compounds. The values of these parameters have been determined by the following procedure. First, we fitted (2) to the experimental data of Festenberg.¹⁵ Then, the real part of the dielectric function was established by the Kramers-Kronig relation¹⁴ and compared to the corresponding experimental data. As a check of the fitting procedure, we required that the calculated energy loss function was also in reasonable agreement with the measured data and that the partial sum rule for valence electrons¹⁶ was satisfied.

Figure 1 shows a comparison of the results of measurement on $\epsilon_1(0, \omega)$, $\epsilon_2(0, \omega)$ and $\text{Im}[-1/\epsilon(0, \omega)]$ for GaP with those calculated using the model. The agreement between theory and experiment for all these functions is qualitatively good. The theoretical results have been calculated based on the best fitted parameters which were determined from comparisons for all these functions and from inspection of the partial sum rule. A better fit resulting to notable changes in the real and imaginary parts of the dielectric function and the energy loss function may not be attainable because experimental data are only available in small energy losses up to about 23 eV, whereas the contribution to the partial sum rule for valence electrons requires the energy loss function extending to much higher energy losses.

The dependence of the energy loss function on momentum transfer is not well known except for the free electron gas system.⁴ Here we have assumed the same relationship for this dependence as applied by Tung and Lin,¹⁷ i.e. $\omega_i(k) = \omega_i + k^2/2$, where k is the momentum transfer. This relationship works correctly at the two ends of $k = 0$ and $k = \infty$ and to the accuracy of k^2 in the expansion of $\omega(k)$.

INNER SHELLS

It is assumed that inner shells of atoms in the solids are essentially unchanged in character from those in free atoms. The local-plasma-approximation, first introduced by Lindhard and Scharff⁸ and later applied by several authors in different applications,¹⁰⁻¹² has been proved to be quite suitable for the treatment of inner shells of atoms. The basic idea of the local-plasma-approximation is quite simple. It assumes that the excitation energies, namely the binding energy and the local-plasma energy, are associated with the electron density distribution at any position in the atom. A physical quantity which depends on the excitation energies is then varying from point to point in the atom. An averaging procedure may be adopted by evaluating the average behaviour of the physical quantity characterized by the atom. In this paper, the differential and total inverse mean free paths for the ionization of inner shells have been estimated based on the local-plasma-approximation. Detailed procedures about this approximation for the evaluation of the generalized oscillator strength¹¹

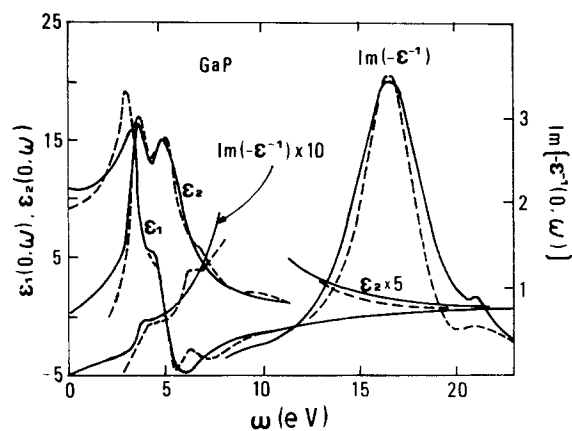


Figure 1. A comparison of experimental¹⁵ (dashed curves) and theoretical (solid curves) results for the real part of the dielectric function $\epsilon_1(0, \omega)$, the imaginary part of the dielectric function $\epsilon_2(0, \omega)$ and the energy loss function $\text{Im}[-1/\epsilon(0, \omega)]$ for GaP.

and the stopping power¹² were presented elsewhere. Applying a similar procedure to the differential inverse mean free path for the ionization of the i th inner shell, we find¹⁸

$$\frac{d\mu_i}{d\omega}(E, \omega) = \frac{\omega_{pi}^2}{2E\omega Z_i} \int_{k_-}^{k_+} \frac{dk}{k} \frac{df_i}{d\omega}, \quad (3)$$

where Z_i is the number of electrons per atom in the i th inner shell and $\omega_{pi} = (4\pi n_i)^{1/2}$ is the plasma frequency of the i th inner shell electrons as if they were free. The generalized oscillator strength per atom of the i th inner shell, $df_i/d\omega$, is given in the local-plasma-approximation as¹¹

$$\frac{df_i}{d\omega} = \frac{\omega Z_i}{\bar{\omega}_{pi} + k^2/2} \delta\{\omega - (\bar{\omega}_{pi} + k^2/2)\}, \quad (4)$$

where

$$\bar{\omega}_{pi} = \{4\pi n_i + \omega_i^2\}^{1/2} \quad (5)$$

and ω_i is the binding energy of the i th inner shell. Carrying out the integration of (3) by noting that $\omega - \bar{\omega}_{pi}$ must fall in the region between $k_-^2/2$ and $k_+^2/2$, one obtains

$$\frac{d\mu_i}{d\omega}(E, \omega) = \frac{\pi n_i(r)}{E\omega(\omega - \bar{\omega}_{pi}(r))}. \quad (6)$$

Note that we have included in (6) the dependence of the electron density and thus $\bar{\omega}_{pi}$ on the electron radius r . The differential inverse mean free path for the ionization of the i th inner shell, given by (6), shows a sharp edge at the binding energy below which no electron can be ionized. It is seen that for large energy losses (6) approaches the non-relativistic Møller formula.¹⁹

Applying the local-plasma-approximation to the inverse mean free path for the ionization of the i th inner shell, we get

$$\mu_i(E) = \frac{\pi n_i(r)}{E} \frac{1}{\bar{\omega}_{pi}(r)} \ln \left[\frac{y_+(y_- + \bar{\omega}_{pi}(r))}{y_-(y_+ + \bar{\omega}_{pi}(r))} \right], \quad (7)$$

where

$$y_{\pm} = \frac{1}{4}(\sqrt{E} \pm \sqrt{E - 2\bar{\omega}_{pi}(r)})^2. \quad (8)$$

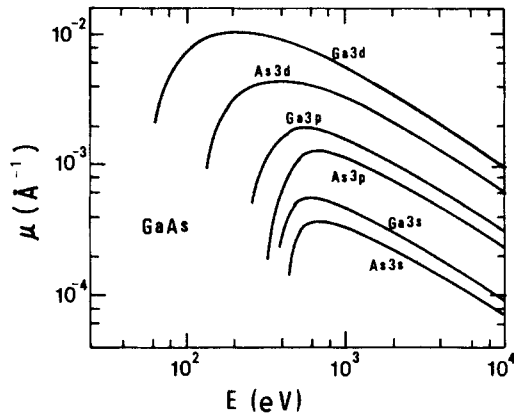


Figure 2. A plot of the electron inverse mean free path in GaAs as contributed by the individual inner shells.

By averaging (7), we obtain

$$\langle \mu_i(E) \rangle = \frac{\pi N}{E} \int \frac{4\pi r^2 n_i(r)}{\bar{\omega}_{pi}(r)} \left[\ln \left(\frac{y_+}{y_+ + \bar{\omega}_{pi}(r)} \right) - \ln \left(\frac{y_-}{y_- + \bar{\omega}_{pi}(r)} \right) \right] dr, \quad (9)$$

where N is the number of atoms per unit volume of the medium. Note that the integration over r in (9) is restricted to the region where $E > 2\omega_{pi}(r)$.

RESULTS AND DISCUSSION

Using (1) and (2) with the fitting coefficients from Ref. 12 and (9) with the electron density distribution from the Hartree-Slater model,⁹ we have calculated the inelastic inverse mean free paths of electrons due to the contributions from the valence band and the inner shells. Figure 2 shows a plot of the individual inner shell contributions to the electron inverse mean free path in GaAs as a function of electron energy. Figure 3 shows the results of the valence band contribution, the inner shell contribution, and the total contribution to the inelastic inverse mean free paths of electrons in GaAs. For comparison we include in the figure the results calculated by Ashley *et al.*²⁰ using a model dielectric function for valence electrons and the classical binary

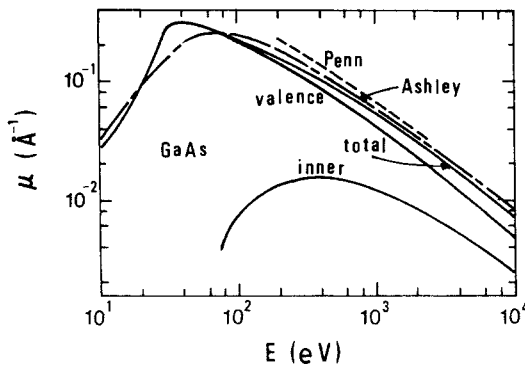


Figure 3. A plot of the inelastic inverse mean free path of electrons in GaAs. The full curves are the results of this work. The results of Ashley *et al.*²⁰ (chain curve) and Penn⁷ (dashed curve) are included for comparison.

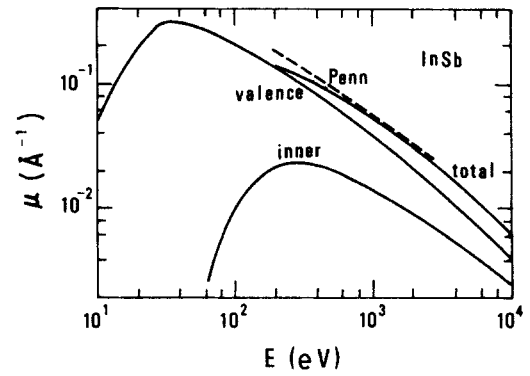


Figure 4. A plot of the inelastic inverse mean free path of electrons in InSb. The full curves are the results of this work. The results calculated using the Penn's model⁷ (dashed curve) are included for comparison.

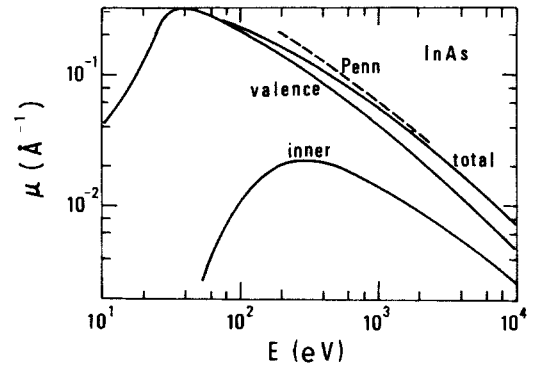


Figure 5. A plot of the inelastic inverse mean free path of electrons in InAs. The full curves are the results of this work. The results calculated using the Penn's model⁷ (dashed curve) are included for comparison.

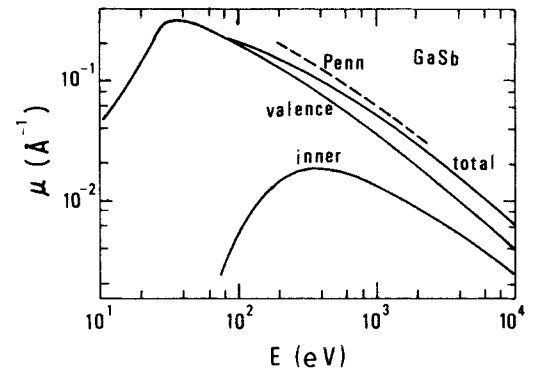


Figure 6. A plot of the inelastic inverse mean free path of electrons in GaSb. The full curves are the results of this work. The results calculated using the Penn's model⁷ (dashed curve) are included for comparison.

collision theory for inner shells, and the model by Penn⁷ using the free electron gas model for all electrons. It is seen that the results of Ashley *et al.* are somewhat larger than the present results for electron energy above about 100 eV. This may be due to the different fitting results on the energy loss function especially for energy losses above 23 eV where experimental data are missing. It may also be due to the different models for inner shells employed in the present work and the work of Ashley

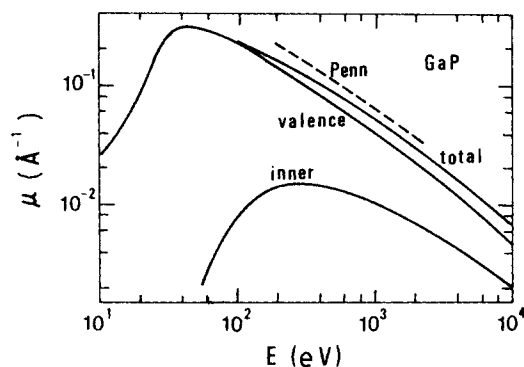


Figure 7. A plot of the inelastic inverse mean free path of electrons in GaP. The full curves are the results of this work. The results calculated using the Penn's model⁷ (dashed curve) are included for comparison.

et al. Penn's model is strictly valid for only the free-electron-like materials which have a simple energy loss spectrum with a single, dominant plasmon peak. With measured optical data available, it is better to calculate the inelastic mean free path by a direct method such as the one presented here.

Figures 4–7 show the results of our calculations for the valence band contribution, the inner shell contribution, and the total contribution to the inelastic inverse mean free paths of electrons in the III–V compounds, InSb, InAs, GaSb and GaP. In all cases, the results

Table 1. Parameters for predicting inelastic mean free paths for electrons with energies from 200 eV to 10 keV from the simple formula $\mu^{-1} = kE^p$.

	200–500 eV (g cm ⁻³)		500–2000 eV		2000–10 ⁴ eV		p
	k	p	k	p	k	p	
GaAs	5.32	0.229	0.635	0.106	0.759	0.0286	0.931
GaSb	5.61	0.501	0.517	0.114	0.755	0.0257	0.951
GaP	4.13	0.186	0.673	0.105	0.764	0.0290	0.934
InAs	5.65	0.257	0.612	0.111	0.747	0.0239	0.949
InSb	5.77	0.442	0.527	0.0839	0.794	0.0241	0.958

obtained from the Penn's model are included for comparison.

It is useful to fit the present results to the simple power formula³

$$\mu^{-1}(E) = kE^p, \quad (10)$$

where both theoretical and experimental evidence²¹ show that p should lie in the range 0.65–0.80 in the energy range from 400 eV to 2000 eV. Our data shown in Table 1, indicate that $\langle p \rangle$ varies from ~ 0.6 for 200–500 eV to ~ 0.76 for 500–2000 eV to ~ 0.95 for 2000–10 keV. These values are in close agreement with the prediction that approximate mean free paths of electrons in the important energy region 400–2000 eV for a wide range of materials are given by the expression $A E^{\langle p \rangle}$, where $\langle p \rangle = 0.73$ (Ref. 3) or 0.75 (Ref. 22) and A is a material dependent parameter.

REFERENCES

1. C. R. Brundle, *J. Vacuum Sci. Technol.* **11**, 212 (1974).
2. H. Tokutaka, K. Nishimori and H. Hayashi, *Surf. Sci.* **149**, 349 (1985).
3. J. C. Ashley and C. J. Tung, *Surf. Interface Anal.* **4**, 52 (1982).
4. C. J. Powell, *Surf. Interface Anal.* **7**, 263 (1985).
5. C. J. Powell, *Surf. Interface Anal.* **7**, 256 (1985).
6. C. J. Tung, J. C. Ashley and R. H. Ritchie, *Surf. Sci.* **81**, 427 (1979).
7. D. P. Penn, *J. Electron Spectrosc.* **9**, 29 (1976).
8. J. Lindhard and M. Scharff, *K. Dan. Vidensk. Selsk. Mat. Fys. Medd.* **27**, 1 (1953).
9. F. Herman and S. Skillman in *Atomic Structure Calculations* Prentice-Hall, New York (1963).
10. W. K. Chu and D. Powers, *Phys. Lett.* **40A**, 23 (1972).
11. C. J. Tung and C. M. Kwei, *Nucl. Instru. Meth.* **B12**, 464 (1985).
12. C. M. Kwei and C. J. Tung, *J. Phys.* **D19**, 255 (1986).
13. C. J. Powell, *Surf. Sci.* **44**, 29 (1974).
14. H. Raether, *Springer Tracts in Mod. Phys.* **88**, 48 (1980).
15. C. V. Festenberg, *Z. Phys.* **227**, 453 (1969).
16. D. Y. Smith and E. Shiles, *Phys. Rev.* **B17**, 4689 (1978).
17. C. J. Tung and C. Lin, *Radiat. Effects*, **80**, 261 (1984).
18. C. J. Tung and R. H. Ritchie, *Phys. Rev.* **B16**, 4302 (1977).
19. C. Møller, *Z. Phys.* **70**, 686 (1931).
20. J. C. Ashley, C. J. Tung, R. H. Ritchie and V. E. Anderson, *Rome Air Development Center Report RADC-TR-76-350*, Griffiths Air Force Base, New York 13441 (1976).
21. C. D. Wagner, L. E. Davis and W. M. Riggs, *Surface. Interface Anal.* **2**, 53 (1980).
22. J. Szajman, J. Liesegang, J. G. Jenkin and R. C. G. Leckey, *J. Electron Spectrosc.* **23**, 97 (1981).